METHODS FOR DETERMINING THE STRUCTURAL AND STOICHIOMETRIC CHANGES OF $Ni(OH)_2$ ELECTRODES DURING POLARIZATION IN ALKALINE ELECTROLYTE

Michael A. Aia and Frederick P. Kober

The Bayside Laboratory, research center of
General Telephone & Electronics Laboratories Incorporated
Bayside, New York

Of the small number of metal oxides that are useful as electrode materials for alkaline batteries, nickel hydroxide combines several desirable characteristics: (1) it is practically insoluble in concentrated alkaline electrolyte, (2) it produces a stable, relatively high potential during discharge, (3) it can be efficiently charged and discharged thousands of times, and (4) it withstands overcharge and overdischarge with relatively little damage. For these reasons, nickel hydroxide is the most commonly used positive electrode material for alkaline cells.

The details of the reactions that occur at the nickel hydroxide electrode in alkaline electrolyte remain poorly defined. It is well established that the starting material has the structure of $Ni(OH)_2$ and is gradually converted to some hydrated nickel oxide (usually written NiOOH) during anodic polarization. Some characteristics of the hydrated nickel oxide obtained by electrolysis of nickel hydroxide are black body color, small particle size, and non-stoichiometric composition. These characteristics present a number of analytical problems, for example, absorption spectroscopy is limited to the infrared, and the small particle size causes diffuse x-ray diffraction patterns. Consequently, the crystal structures of the hydrous oxides of nickel have not yet been determined. In the present work, physical, chemical, and electrochemical approaches were used to obtain information on the structure, composition, and hydration states of nickel hydroxide as a function of its oxidation state.

Experimental Procedures

Electrodes were prepared by impregnating porous sintered nickel plaques of 80 percent porosity with $Ni(OH)_2$. The plaques were dipped in nickel nitrate solution and then cathodically polarized in concentrated KOH solution.[5] The impregnated electrodes were charged and discharged several times before the nickel hydroxide was anodized to different states of charge. Before analysis, electrodes were washed and dryed in nitrogen or vacuum and then ground with a mortar and pestle. Iodometric analysis for active oxygen in the ground powders indicated that the preparative treatment did not significantly decompose the samples. Active oxygen was determined by dissolving 0.1 g of sample in a sodium acetate-buffered solution of acetic acid containing potassium iodide and starch indicator solution; the iodine liberated was titrated with 0.1 N sodium thiosulfate solution. The methods used for further treatment and analysis of the samples, as well as the principal results obtained, are summarized in Table I.

TABLE I

Methods Used and Principal Information Obtained

Technique	Principal Results
X-ray Powder Diffraction	Overall structure and particle size.
Hydrothermal Treatment	Improved crystals for structural studies.
Infrared Absorption	Vibrational spectra of protons.
Thermal Decomposition (DTA and TGA)	Nature of hydration states.
Mass Spectrometry	Analysis of thermal decomposition products.
Chemical Analysis (% Ni, K, H_2O, O)	Composition and stoichiometry.
Constant Current Polarization	Electrical capacity and potential.

Results and Discussion

Considerable information can be obtained from x-ray powder diffraction patterns, but the results are often ambiguous in the absence of supporting data from single crystal work. In spite of all the compositions and x-ray diffraction patterns that have been reported for oxides and hydrous oxides of nickel, only the structures of NiO (rocksalt) and $Ni(OH)_2$ (brucite) have

een defined. Even $Ni(OH)_2$ has never been studied in detail probably because of the difficulty i obtaining single crystals. Some structural assignments have been made from x-ray powder iffraction analysis: $Ni(OH)_2$ has the hexagonal layer structure of brucite,[4,13] and the space roup is D_{3d}^3 - $P\bar{3}m1$. The overall structure is composed of complete layers of NiO_6 octahedra, s shown schematically in Fig. 1. The D_{3d} site symmetry and layering of the Ni and O atoms t the unit cell can be seen in Fig. 2. Adjacent OH groups are free, i.e., not connected by ydrogen bonds.

he x-ray powder diffraction patterns of nickel hydroxide, as precipitated and in various tates-of-charge, are summarized in Fig. 3. The lattice becomes distorted, and the patterns ose some of their features as the oxidation state of nickel hydroxide is increased. A shift to arger values for the d_{hkl}-spacing of the (001) reflection occurs during oxidation and provides direct measure of the expansion of the lattice in the c-direction of the unit cell (Fig. 2). his expansion has also been observed by Harivel and co-workers.[7] A more quantitative xplanation of the structural disorder occurring during anodic oxidation of $Ni(OH)_2$ was given ecently by R. Ritterman and co-workers.[15] As shown in Fig. 3 lattice distortion eventually auses the appearance of a new phase, termed $Ni_2O_3 \cdot H_2O$ by Cairns and Ott,[4] γ-NiOOH by lemser and Einerhand,[6] and alpha-phase by Tuomi.[18] A major characteristic of this highly xidized phase is the diffraction band at d = 6.9 Å. Sharp x-ray diffraction patterns for $Ni(OH)_2$ nd $Ni_2O_3 \cdot H_2O$ treated hydrothermally in 10 N KOH solution for several days, also shown in ig. 3, indicate the utility of the hydrothermal method for obtaining materials suitable for tructural studies.[1] The crystal structure of the material obtained by hydrothermal treatnent of $Ni_2O_3 \cdot H_2O$ is still under study.[3] In agreement with crystal field calculations,[12] the verall symmetry is lower than hexagonal.

nfrared spectroscopy was a useful complement to the x-ray diffraction analysis because of ts ability to detect changes in the bonding of protons and water in the lattice. As can be seen n Fig. 4, infrared spectra show the OH vibrations characteristic of non-hydrogen-bonded OH roups in both the starting $Ni(OH)_2$ and in the discharged electrode. As the oxidation state f the nickel hydroxide is increased, the intensity of the free OH vibrations decrease, while vibrations due to hydrogen-bonded water appear in the spectra.[9,10]

ifferential thermal analysis (DTA) curves, shown in Fig. 5, established that the energy required for thermal decomposition of Ni-OH groups decreases continuously as $Ni(OH)_2$ is brought to higher oxidation states.[2] The relative areas under the second peak are indicated. From Fig. 5 it can also be seen that the loosely bound water always found in precipitated $Ni(OH)_2$,[2,10] (approximately 0.3 mole H_2O per mole $Ni(OH)_2$ is more discretely bound in charged electrodes, especially after the structural change to $Ni_2O_3 \cdot H_2O$ (γ-NiOOH) occurs. For example, compare the first peaks of curves A and J.

Chemical analysis showed that the decrease in hydroxyl water content is accompanied by a corresponding gain in "active oxygen," [O], content. The sum of H_2O and [O] remains essentially constant[2] at 1.3 moles per mole NiO, as shown in Table II.

TABLE II
Chemical Analysis of Dried Nickel-Hydroxide-Impregnated Electrodes in Various States-of-Charge

	Moles per Mole Ni		
State-of-Charge	K	[O]	H_2O
Over discharged	<0.01	0.10	1.20
68% Charged	0.08	0.41	0.84
100% Charged	0.14	0.55	0.70
660% Charged	0.16	0.81	0.50

The constancy of the total oxygen content of vacuum-dried samples was confirmed by neutron-activation analysis for oxygen which showed 33.6 weight percent in the discharged nickel hydroxide and 33.8 weight percent in the overcharged material. The electrochemical equivalent of the active oxygen found by analysis was in quantitative agreement with that calculated for the amount of charge passed up to about 1.2 Faraday per g.at Ni. For example, after the passage of 1 Faraday per g.at Ni the active oxygen content was 0.5 g.at per g.at Ni.

Table II also shows that the potassium ion content of the nickel hydroxide increases continuously throughout oxidation in KOH electrolyte. The take-up of potassium ions is reversible, and practically no K^+ remains in the lattice after discharge.[2] The sorption occurs, to a lesser degree, in NaOH solution but not in LiOH where only 20 ppm Li was found after extended anodic polarization. The sorption of alkali metal cations, which is apparently contrary to the flow of current, seems to play an important role in the rate and extent of structural transformation of $Ni(OH)_2$ to $Ni_2O_3 \cdot H_2O$ (γ-NiOOH). The tendency for structural conversion decreased in the order $K^+ > Rb^+ > Na^+ > Cs^+ > Li^+$, as will be described in detail in a subsequent paper.[3] There was no evidence in x-ray patterns for the formation of γ-NiOOH in LiOH solution, which agrees with Tuomi's results.[18] Furthermore, infrared absorption indicates that the OH groups of the solid phase remain free throughout oxidation in LiOH, and there is no evidence for the hydrogen bonding that occurs in KOH and NaOH.

Thermogravimetric analysis (TGA) shows that about 10 percent H_2O is removed from the charged material up to a heating temperature of 150°C, as shown in Fig. 6(a). Heating to higher temperatures causes the layer lattice to break down, and NiO is observed in the x-ray diffraction patterns (see top of Fig. 6). Above 250°C the surface area of the material begins to decrease rapidly, as shown in Fig. 6(b). The surface areas were calculated from line widths on the x-ray diffraction pattern, using the method described by Keeley.[8] The line at d = 6.9 Å was used for γ-NiOOH up to 140°C, and the line at d = 2.41 Å was used for NiO from 140° to 400°C; line widths were compared to that of the Ni spacing peaking at d = 1.762 Å. Using gas adsorption, Salkind and co-workers[16] reported values of 61-80 m^2/g for the active material in discharged nickel hydroxide electrodes; in charged electrodes, the surface area was about 10 percent higher.[17] The loss of surface area starts at higher temperatures than the loss of electrochemical capacity stored by the charged material, as shown in Fig. 6(c). Infrared analysis has shown that the capacity loss caused by thermal treatment of charged electrodes is accompanied by a corresponding loss in the intensity of absorption due to "hydrogen-bonded water" at 580 cm^{-1}.[11] In discharged electrodes the thermally induced loss of electrochemical activity is directly related to the loss in intensity of free OH vibrations in the infrared spectra.[10] The gases released during thermal decomposition were analyzed with a mass spectrometer.[3] The results for a charged material corresponding to NiOOH show that oxygen, as O_2, was released from previously vacuum dried, charged material in appreciable amounts only above 200°C; the rate of evolution of O_2 was fastest at about 250°C. X-ray diffraction data showed that above 250°C the NiO became much better crystallized and the surface area decreased rapidly. From TGA, the amount of O_2 plus residual H_2O evolved from 150° to 400°C was close to 9 percent of the starting weight; the theoretical [O] content of NiOOH is 8.7 percent.

Summary

A wide variety of standard methods of analysis were used to study changes that occur in the structure and chemical composition of nickel hydroxide electrodes during anodic polarization in concentrated aqueous solutions of Group I metal hydroxides. X-ray diffraction patterns indicate the general nature of the distortion and expansion of the unit cell, but give no information on the hydration states. Infrared absorption spectra reveal the continuous alteration of hydroxyl sites and the formation of hydrogen-bonded water when $Ni(OH)_2$ is anodized in 7N KOH. Electrochemical activity was found to be closely related to the quantity of hydroxyl sites in the solid phases. Thermal decomposition analysis shows that the start of loss of electrochemical activity is accompanied by the formation of NiO and the loss of water of constitution, but not the loss of surface area.

REFERENCES

1. Aia, M. A., J. Electrochem. Soc. 113, 1045 (1966).
2. Aia, M. A., Battery Symposium of the Philadelphia Meeting of the Electrochemical Society, Abstract No. 16, October 1966; submitted to J. Electrochem. Soc.
3. Aia, M. A., to be published.
4. Cairns, R. W. and Ott, E., J. Am. Chem. Soc. 55, 527 (1933).
5. Fleischer, A., J. Electrochem. Soc. 94, 289 (1948).
6. Glemser, O. and Einerhand, J., Z. Anorg. u. Allgem. Chem. 261, 43 (1950).
7. Harivel, J. P., Morignat, B., Labat, J. and Laurent, J. F., 5th International Power Sources Symp., Brighton, September 1966.
8. Keeley, W. M., Anal. Chem. 38, 147 (1966).
9. Kober, F. P., J. Electrochem. Soc. 112, 1064 (1965).
10. Kober, F. P., 5th International Power Sources Symp., Brighton, September 1966.
11. Kober, F. P., J. Electrochem. Soc., to be published in early 1967.
12. Kober, F. P. and Aia, M. A., to be presented at Dallas Meeting of the Electrochem. Soc., May 1967.
13. Natta, G., Rend. accad. Lincei 2, 495 (1925).
14. Pauling, L., The Nature of the Chemical Bond, 3rd ed., p. 557 Cornell University Press, Ithaca, New York (1960).
15. Ritterman, P., Lerner S., Vaughan, P., and Seiger, H. N., Battery Symposium of the Philadelphia Meeting of the Electrochem. Soc., Abstract No. 15, October 1966.
16. Salkind, A. J., Cannin, H. J., and Block, M. L., Electrochem. Technol. 2, 254 (1964).
17. Salkind, A. J. and Bodamer, G. W., Batteries, 2, D. H. Collins, Editor, pp. 55-62 Pergamon Press, New York (1965).
18. Tuomi, D., J. Electrochem. Soc. 112, 1 (1965).

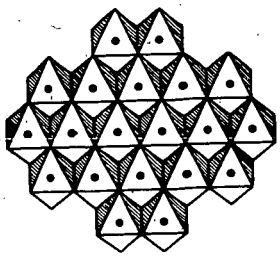

Fig. 1. Schematic diagram of the brucite layer lattice showing the complete layers of NiO_6 octahedra.

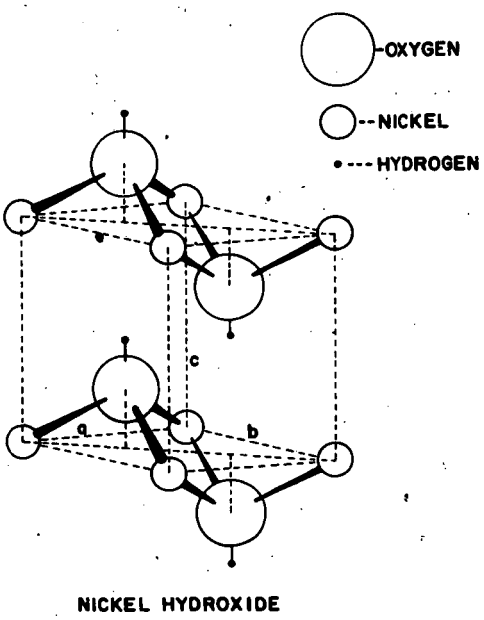

Fig. 2. The unit cell of $Ni(OH)_2$ showing the D_{3d} site symmetry.

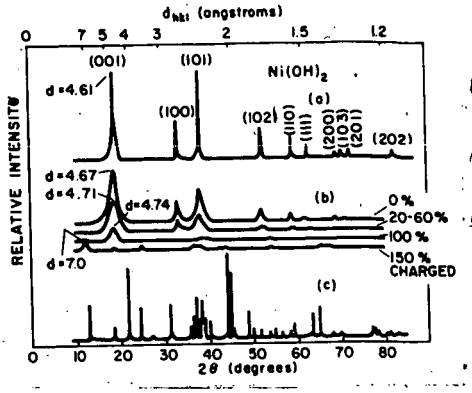

Fig. 3. X-ray powder diffraction diagrams; (a) Hydrothermally treated Ni(OH)2, (b) Electrodes at various states of charge, (c) Hydrothermally treated $Ni_2O_3 \cdot H_2O$.

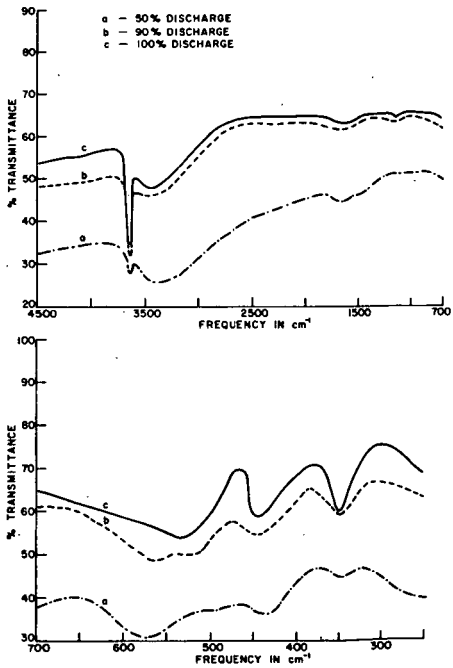

Fig. 4. Infrared absorption spectra of electrodes at various stages of discharge

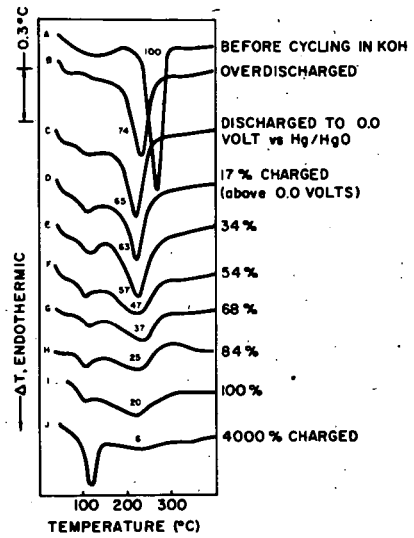

Fig. 5. Differential thermal analysis of electrodes at various states of charge.

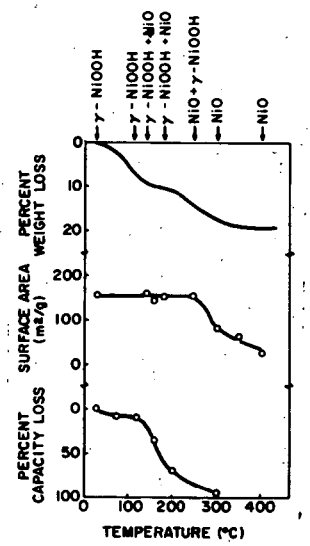

Fig. 6. Weight loss, surface area, and electrical capacity loss as a function of heating temperature.